atmosphere

MDPI

Article

Topoclimatic Zoning and Representative Areas as Determined by an Automatic Weather Station (AWS) Network in the Atacama Region, Chile

Donna Cortez [1,2], Rodrigo Padilla [3], Sebastián Herrera [1], Juan Manuel Uribe [2] and Manuel Paneque [2,*]

1 Bionostra Chile Research Foundation, Almirante Lynch 1179, San Miguel, Santiago 8920033, Chile; dcortez@bionostra.com (D.C.); sherrera1k@gmail.com (S.H.)
2 Department of Environmental Sciences and Natural Resources, Faculty of Agricultural Sciences, University of Chile, Santa Rosa 11315, La Pintana, Santiago 8820808, Chile; jmuribe@renare.uchile.cl
3 Oficina Servicios Climáticos, Sección Climatología, Subdepartamento Climatología y Meteorología Aplicada, Dirección Meteorológica de Chile, Av. Portales 3450, Estación Central, Santiago 9170018, Chile; rodrigo.padilla@meteochile.cl
* Correspondence: mpaneque@uchile.cl; Tel.: +56-2-2978-5863

Received: 7 May 2020; Accepted: 8 June 2020; Published: 9 June 2020

Abstract: Climate information is crucial to the management and profitability of key development sectors involving agriculture, hydrologic resources, natural hazards, and energy. Climate knowledge, real-time weather information, and climate predictions reliability all contribute to the planning and management of socioeconomic activities and sustainable development. Automatic weather stations (AWSs) are remotely operated and facilitate the recording of meteorological information for unoccupied and out-of-reach areas. However, the representative area of the Atacama region is unknown, whose uniqueness is largely determined by the topography of the terrain. This paper describes the topoclimatic zoning of the Atacama region, based on the identification of homogeneous climatic and topographic areas, using climatic information, principal component analysis, and cluster analysis. Topoclimatic zoning was used to determine the representative area of the AWSs. Sixty-one regional topographic units were identified as equivalent to the representative area of the AWS. The directly represented area was estimated at 2365 km^2 (3.13% of the regional total), the indirectly represented area was 8725 km^2 (11.53%), and the unrepresented area was 64,561 km^2 (85.34%). This large unrepresented area displays potential zones for future AWS installations, which can improve both the efficiency of the regional meteorological network and access to quality climate information.

Keywords: topoclimatic zoning; automatic weather stations (AWS); principal component analysis (PCA); cluster analysis (CA)

1. Introduction

Climate studies are of scientific, environmental, and economic interest, because they determine the distribution and behavior of organisms that influence various productive activities, such as those involving agriculture, hydrologic planning, and energy efficiency [1]. Climate studies require meteorological information that is accurate, extensive, and constantly accessible [2]. Nevertheless, the lack of a homogeneously distributed weather station network in Chile that represents climatic variability complicates regional and national climate studies [3]. This limits the large-scale use of precise climatic information [4].

Automatic weather stations (AWSs) allow the fulfillment of climate studies by remotely recording the climate conditions twenty-four hours a day [5,6]. AWSs deliver high-frequency data in real time and can be installed in remote and uninhabited zones [2]. The Meteorological Station Network

(MSN) was installed and expanded using the installation criteria, according to the requirement of the installation agency, as opposed to topographic singularities, which would provide territorial representativeness [7,8]. In Chile, information regarding the representative areas of AWSs is scarce, such that territorially distributed climatic variables are unknown [9,10].

Climates assume local characteristics that can be influenced by numerous factors, including the topographic form [11]. Therefore, relief plays a significant role in climate distribution, because it constitutes a barrier against oceanic influences. Temperatures decrease as altitude increases, while shadows from transverse and longitudinal mountains are projected over valleys, affecting daily temperatures and annual fluctuations [12,13]. The Atacama surface is defined by the extreme roughness of its relief, due to topography associated with the mountain and foothill systems (40.3%), pampas (32.7%), and high-plateau basins (18.5%) [13].

The Atacama region is of special interest, due to its climatic and topographic complexities, since it is considered a transition zone between the hyper-arid climate of the Antofagasta region and the semi-arid Mediterranean climate of Coquimbo [13]. In addition, the region contains important altitude differences. The highest altitudes are found at the national level in the Andean area and the occurrence of the first transverse valleys is also observed between the Copiapó and Aconcagua river basins (Valparaíso region) [9]. This condition influences the wealth of natural resources found in the region and the development of various productive activities. The main activities are mining, which contributes 38.4% of the regional GDP; agricultural activities that contribute 4.4%; and tourism that contributes 18.8% [14]. Thus, it is necessary to obtain quality climate information for the entire territory, which allows support for decision-making that promotes productive development and conservation of natural resources.

In the Atacama region, the available real-time weather information is generated by 16 AWSs [15] for an approximate area of 75,000 km^2 [16], which represents 53.3% coverage of the regional extension according to World Meteorological Organization (WMO) criteria [17]. The WMO suggests that, for mountainous terrain, there should be at least one pluviometer for every 2500 km^2 [17]. However, this area depends on the topography, especially for extreme rugosity [9]. The area influenced by each weather station (WS) installed in the region is unknown, as is the unrepresented area. Understanding the WS influence area allows the identification and quantification of the territory surfaces, which are where current meteorological data are collected [18]. This knowledge enables the validation of climatic models by comparison with these point data, while dynamic climate models are generated for cells in a grid model [19].

The determination of a homogenous climatic zone has been the subject of global [20–32] and nationwide studies [3,10,33–39]. In these studies, climatic determinations change according to the zoning method employed, the cartographic scale, and available technology at the time of generation [37]. Complex statistical procedures have recently been used to group regional climates and define similar climate areas, such as cluster analysis (CA) [23,40–42] and supervised and unsupervised classification [43].

Morales et al. (2006) [37] developed the edaphoclimatic zoning of the Coquimbo region and used 17 thermal, hydric, and energy climate variables, distributed according to a multi-regressive method. This included topographic variables, such as latitude, longitude, distance to the sea, and distance to the hydric network. The identification of homogeneous climatic areas was accomplished using CA with the K-means algorithm, which unified the resulting cartography with the regional soil usage. Uribe et al. (2012) [3] generated cartographies of climatic variables via an expert layout using AWS data (See Supplementary Materials). This indicates that the vegetation cartography and topographic parameters, such as latitude, longitude, height, and exposure, were employed as a reference. The variables were spatialized through the natural-neighbor interpolation. Santibáñez et al. (2017) [38] conducted an agro-climatic zoning of Chile using a nonlinear multiple regression approach, which considered meteorological station data. The elevation, latitude, and distance to the sea were used to distribute the variables, while CA identified the isoclimatic zones.

In this study, we conducted topoclimatic zoning of the Atacama region. Areas were defined according to a spatial scale that established relationships and found patterns among the various climatic and topographic variables that characterize a certain terrain [11]. The effects of spatial variability at a local climate scale were determined via independent climatic and topographic classifications made with principal component analysis (PCA) and CA [13]. This zoning can be replicated in any other region using layers of climatic variables previously elaborated. These can be different to the variables used in this study, which is important, because this requires fewer resources than other analyses.

The topoclimatic zoning of Atacama was used to estimate the representative area of the AWS network present in the region. This differentiates this study from previous investigations that were not developed for this purpose. For this reason, the present study has special relevance, considering the lack of planning involved in the installation of AWS networks.

This paper is structured as follows: the Data and Methods section describes the basic climatic and topographic information, and the method used for zoning and estimating representative areas of AWSs in the study; the Results section presents the climatic, topographic, and topoclimatic cartographies generated by zoning, and the areas represented by AWSs are identified; the Discussion presents a discussion of the methodology used and comparisons of the results with those of similar studies; and the Conclusions summarize the findings of the study and its scope.

2. Data and Methods

2.1. Study Area

The study area is in the Atacama region, ranging between 25°17′ and 29°11′ S and 68°17′ W towards the Pacific Ocean, with an area of approximately 75,652 km^2 (Figure 1) [44].

To the north, the climate of the Atacama region borders the hyper-arid zone of the Antofagasta region, which is influenced by the trade wind belt from the Amazonas. This generates summer precipitation at high altitudes in the Los Andes Mountains. The southern border is with the Mediterranean semi-arid zone of the Coquimbo region, where winter rains occur, caused by final influences of the westerlies wind belt. These winds transport frontal systems and migrating low pressure from the southwest. In addition, the subtropical anticyclone from the South Pacific, a prevailing feature at this latitude [13,45], influences the climate.

The Los Andes mountains in the Atacama region generate a "rain shadow" effect, which blocks precipitation from the Amazonas. In the west, the cold Humboldt stream and upwelling of deep waters reduces the water evaporation capacity of the Pacific Ocean into the atmosphere. This results in scarce precipitation with values between 4.0 and 169 mm year^{-1} [3].

According to its precipitation and temperature conditions, the Atacama includes four climate units based on the Köppen classification [46,47]: Coast Desert with Abundant Cloudiness (BWn), Transitional Desert Climate (BWi), Mountain Cold Desert (BWk'G), and High Mountain Tundra Climate (EB), distributed from west to east, with a clear altitudinal progression [13].

The topography of the Atacama region is characterized by a system of high plateaus, which alternate between the Los Andes foothills and mountains to the north and south, respectively, and transverse valleys between the Copiapó (Atacama) and Aconcagua river basins (Valparaíso) [9]. In the Atacama region, there are two distinct hydrographic sectors: north of the 27° S parallel, where precipitation is scarce (approximately 1.7 mm year^{-1}), which represents an arheic region, and south of the same parallel, where precipitation is slightly higher (up to 42 mm year^{-1}), which allows for the development of an exorheic zone with pluvial and snow-derived rivers [9,13].

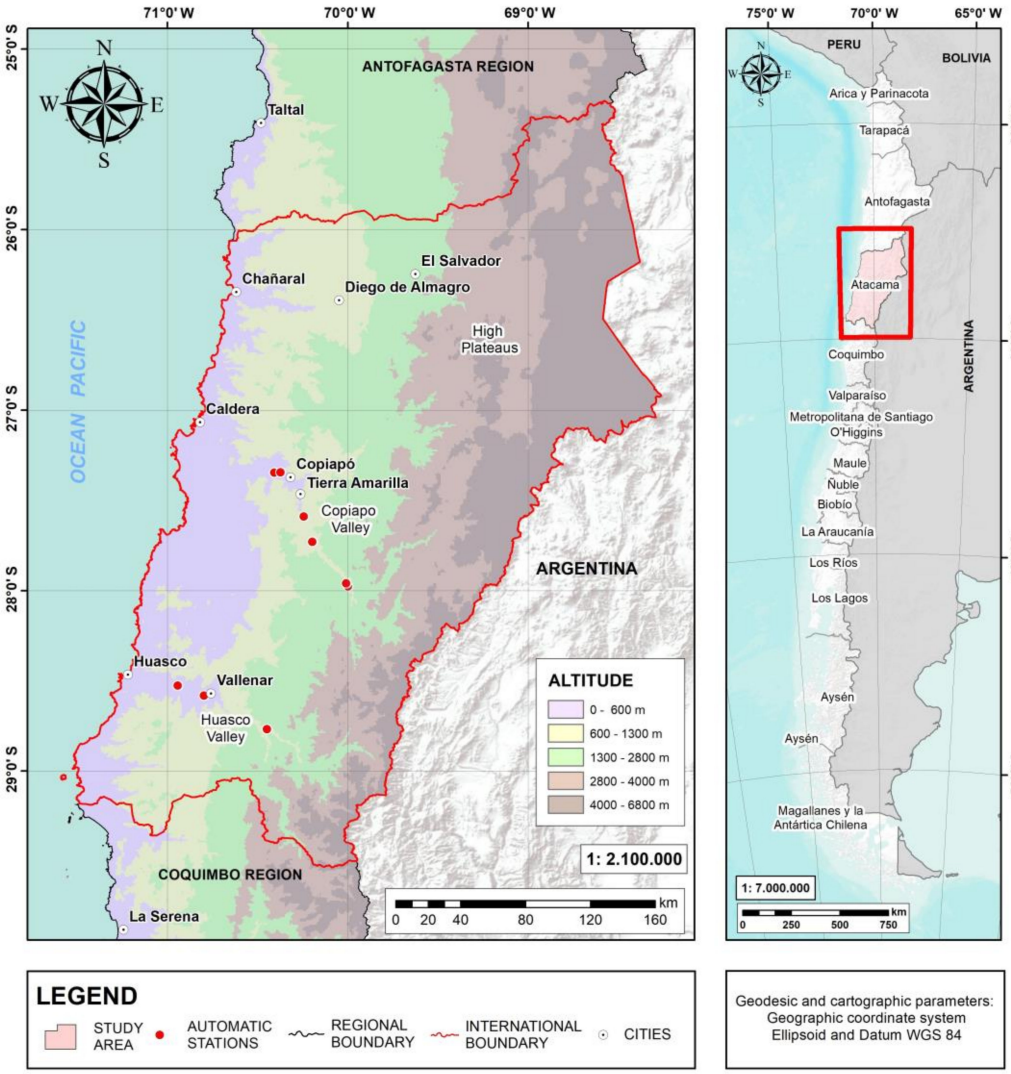

Figure 1. Study area: the Atacama region, Chile, with the automatic weather stations (AWSs) analyzed in this work.

2.2. Basic Climatic and Topographic Characteristics

The homogeneous climatic areas were delineated using the digital layers in a raster format of the 26 variables elaborated in the Atlas Bioclimático de Chile as a basis (Table 1A) [3], with a resolution of 90 m (1:250,000 scale). Uribe et al. (2012) [3] documented the basic climate variables (temperature and precipitation) using mapped isolines, which were interpolated using the natural-neighbor method. The derived variables were then calculated, with the basic variables as inputs (View S1: Methodology for obtaining climatic variables from the Atlas Bioclimático de Chile). It is important to note that the summer and winter severity include the thermal amplitude between the summer and winter seasons, using the maximum average temperature statistics for January and July, and the minimum average temperatures for the same months. The registered thermal amplitude shows the degree of severity or intensity of the effects of continentality or amount of coastal influence that characterize a given climate or location.

Table 1. Climatic and topographic variables used in the Topoclimatic zoning of the Atacama region.

Variable	Acronym
(A) Climatic Variables	
Water deficit	DEFH
Degree days	DGAG
Annual degree days	DGAN
Evapotranspiration in January	ETP_E
Evapotranspiration in July	ETP_J
Water surplus	EXCH
Relative humidity in January	HR_E
Relative humidity in July	HR_J
Cold hours	HRSF
Aridity index	IARI
Humidity index in January	IH_E
Humidity index in July	IH_J
Humid period	PERH
Dry period	PERS
Frost-free period	PLH
Annual precipitation	PPA
Solar radiation in January	RS_E
Solar radiation in July	RS_J
Summer severity	SEV_EST
Winter severity	SEV_INV
Average temperature in January	TMA_E
Average temperature in July	TMA_J
Maximum temperature in January	TMAX_E
Maximum temperature in July	TMAX_J
Minimum temperature in January	TMIN_E
Minimum temperature in July	TMIN_J
(B) Topographic Variables	
Elevation	
Slope	
Convexity	
Rugosity	

Four variables were considered for the zoning of homogeneous topographic areas in this study (Table 1B). These variables were extracted via a digital elevation model (DEM) taken by the Shuttle Radar Topography Mission (SRTM) sensor with a resolution of 30 m in raster format [48]. A different resolution to that of the climatic layers was employed to obtain more details and sensitivity in the zoning. The topographic variables used are representative of the regional topography, and can be applied as direct or indirect local climate estimators [9,13,49].

The PCA and CA were performed using the RStudio statistical software. The values for the digital layers were extracted from a geographic grid the size of the Atacama region with a resolution of 1.0 km [10,50], corresponding to an analysis on a local scale (0.1 to 3.0 km) [51]. The average values for

the pixels in each grid were obtained from the layers of the climatic variables and average elevations. The maximum value of the slope was used to model the greatest changes in the relief [52], while the standard deviations of the convexity and rugosity were used to evaluate the heterogeneity of those parameters in the terrain [53], which were obtained using the topographic variables.

2.3. Climatic and Topographic Zoning

The climatic and topographic zones with homogenous characteristics were determined using PCA and CA [24,25,54–56].

2.3.1. PCA

PCA was applied to the climatic variables obtained by Uribe et al. (2012) [3], beginning with the 1 km grid to reduce the variable set where there was a high correlation between variables. Correlation was determined using a Kendall correlation matrix [57] and the Kaiser-Meyer-Olkin (KMO) multicollinearity test. In both cases, values greater than 0.6 indicated a high correlation between the variables and redundant information in the dataset [24,58], justifying the need to execute a PCA. In the PCA, each variable in a component was grouped according to the best linear combinations of the variables, which allows less important components in the data group to be eliminated [29,59]. This avoids information repetition and simplifies processing [60]. PCA creates components, different to the original variables, and each contributes to the principal components by assigning different loads or weights. These components contain the most important information from the complete original data sample [40]. The first components have higher values as they maintain a higher sample variability [56,61].

The principal components were selected according to the following criteria: (1) components that express a higher percentage of the total variance; (2) establishing a threshold collected by these components in which the variance should be between 70 and 90% [62]; (3) applying the Kaiser rule regarding the conservation of components with eigenvalues greater than the unit [63]; and (4) building a scree plot that shows variance versus component number, which dismisses the factors below the graph inflexion point [64,65].

When selecting the principal components, we attempted to obtain a high loading value with more than one component (higher than 0.6), or components with a low loading compared with all measured variables, such that these components were subsequently rotated using the varimax orthogonal rotation method [66]. The rotation was performed to obtain strong loadings between each variable, and one other component to determine the representativeness of each component, according to the prevailing type of variable in each [67].

This component selection was validated using the root mean square error of approximation (RMSEA) [68], where a residual statistical value threshold of 0.05 was employed [69].

2.3.2. CA

CA was used to form groups of equal variables, beginning with the similarities and dissimilarities between the PCA data [70] to achieve the highest homogeneity within each group and the highest heterogeneity between them [71]. A non-hierarchical grouping method was used given its low computational cost and suitability to large data matrices. A cluster number was defined a priori to classify the resulting PCA information [72].

Each cluster datum was assigned using the K-means algorithm [73] by maintaining the sum of squares data inside the clusters and the minimum. This distance was estimated using the Euclidian distance method [37,74]. Centroids were randomly defined for each cluster and each datum was considered to be associated with the closest centroid when using the Euclidian distance.

New centroids were then randomly selected and the distances recalculated, which reassigned the datum to a new cluster. This cycle was repeated ten times [74,75]. The data groupings were spatialized to generate climatic and topographic zoning cartographies.

2.4. Topoclimatic Zoning

The climatic and topographic cartographies were combined, assigning a specific value to each unique combination of elements, which allowed the identification of homogeneous topoclimatic areas in the Atacama region. Less than 0.8% of areas were eliminated from the regional surface area, as they were considered non-significant at the study analysis scale.

A climatic description was created using each topoclimate identified according to six climate variables that characterize the key aspects of the regional climate: three from the thermal regime (TMAX_E, TMIN_J, and PLH), representing the annual thermic amplitude condition, and extreme thermic events. Another three variables were identified from the hydrological regime (ETP_E, ETP_J, and DEFH), which correspond to the evapotranspiration rates of the warmer and colder months and water availability.

2.5. AWS Representation Area in the Atacama Region

Representative area estimation considered the regional topoclimatic delimitations and geographic coordinates of 16 AWSs, distributed throughout the Atacama region (Table 2). The representative area was estimated by considering only the AWSs. In comparison with the conventional meteorological stations, these presented both accurate locations and security in terms of data reading [76], which is of significant relevance to a local study. The representative areas were identified as: (1) zones with direct representativeness (homogeneous areas that contain one or more AWSs that compile meteorological information at its location); (2) areas with indirect representativeness (meteorological information was not compiled by the AWSs, but can be standardized using direct-representation area information, because both have the same climatologies); and (3) areas without representation (corresponding to zones without an AWS and with different homogeneous areas than those that are represented), which can be potentially considered to improve the regional AWS coverage.

Table 2. Automatic weather station (AWS) locations in the National Meteorological Network (NMN), which was installed in the Atacama region, and was used for influence-area estimation, according to topoclimatic zoning.

AWS	District	Latitude	Longitude	Altitude (m)
Copiapó	Copiapó	−27.35	−70.41	342
Bodega	Copiapó	−27.34	−70.37	347
Jotabeche	Tierra Amarilla	−27.59	−70.24	599
Hornitos	Tierra Amarilla	−27.73	−70.20	769
Tranque Lautaro	Tierra Amarilla	−27.98	−70.00	1132
Amolana Copiapó 2	Tierra Amarilla	−27.96	−70.01	1091
Iglesia Colorada	Tierra Amarilla	−28.15	−69.89	1517
Altar de la Virgen	Tierra Amarilla	−27.99	−69.98	1115
CE Huasco	Vallenar	−28.58	−70.80	465
Cachiyuyo	Vallenar	−29.06	−70.90	950
Alto del Carmen	Alto del Carmen	−28.77	−70.45	822
La Copa	Caldera	−27.35	−70.62	188
Falda Verde	Chañaral	−26.3	−70.62	127
Vallenar	Freirina	−28.53	−70.94	230
Freirina	Freirina	−28.51	−70.94	92
Vallenar	Freirina	−28.53	−70.94	226
Punta Lobos	Huasco	−28.30	−71.18	30

3. Results

3.1. Climatic and Topographic Zoning

3.1.1. PCA of Climatic and Topographic Variables

The climatic variables showed a Kendall collinearity matrix, in which 185 of the 325 values were equal to or greater than 0.6, with a main KMO multicollinearity factor of 0.92. The topographic variables showed three of the six values equal to or greater than 0.6, with a multicollinearity factor of 0.73. Both variables indicate that unnecessary information was present within the original data. Hence, the volume of the information was reduced using the PCA. In the PCA, three components were selected to represent the 26 climatic variables, which described 89.96% of the accumulated variance (Table 3) (Figure 2a). The four topographic variables were represented by three components that contained approximately all the original information, i.e., 97.97% of the accumulated variance. The third topographic component was integrated in the selection of components, because it contained 14.3% of the topographic information (Table 3) (Figure 2b).

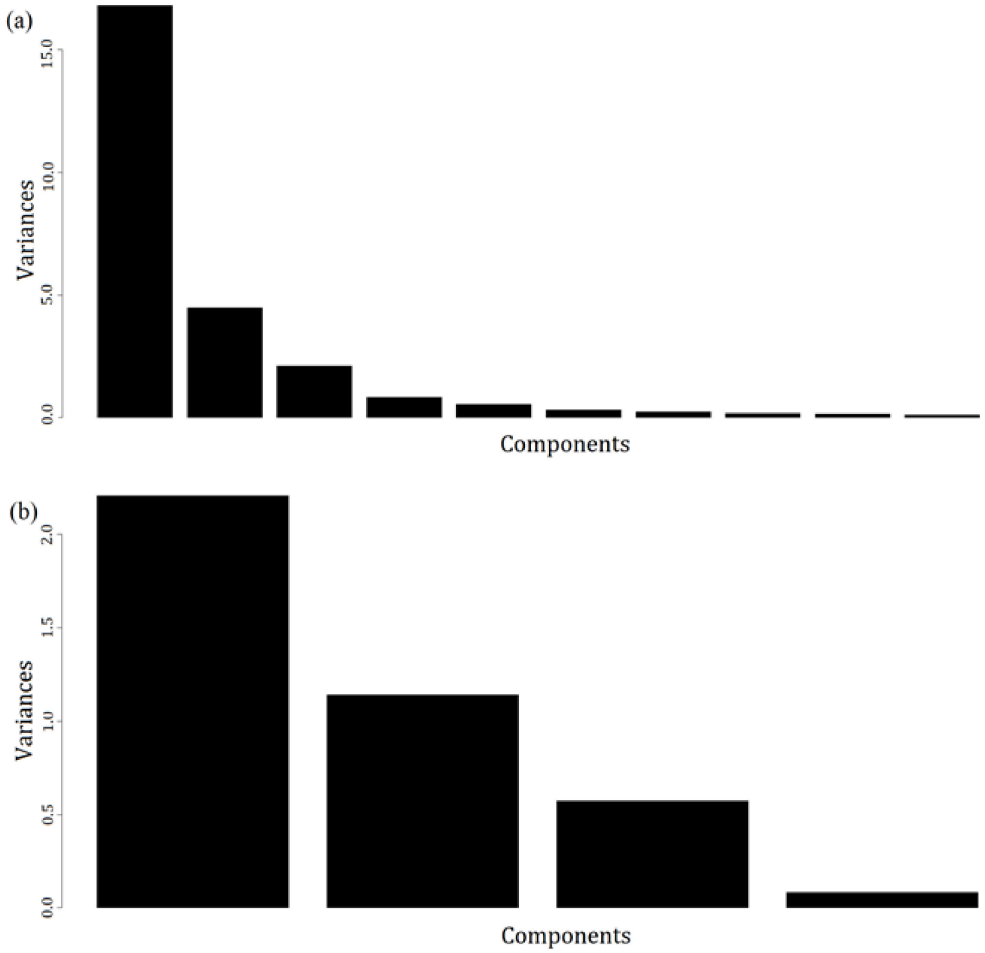

Figure 2. Scree plot that shows the variance in the principal components for (**a**) 26 climatic variables in the Atlas Bioclimático de Chile (Uribe et al., 2012) [3] and (**b**) four topographic variables obtained through a digital elevation model (DEM) in the Atacama region.

The selected climate and topographic PCs were rotated, because the third climatic and topographic components showed low loadings with all the variables, while the climate variables, i.e., ETP_E and IH_J, were characterized by a loading value greater than 0.6, with more than one component (see Figures 3a–c and 4a–c).

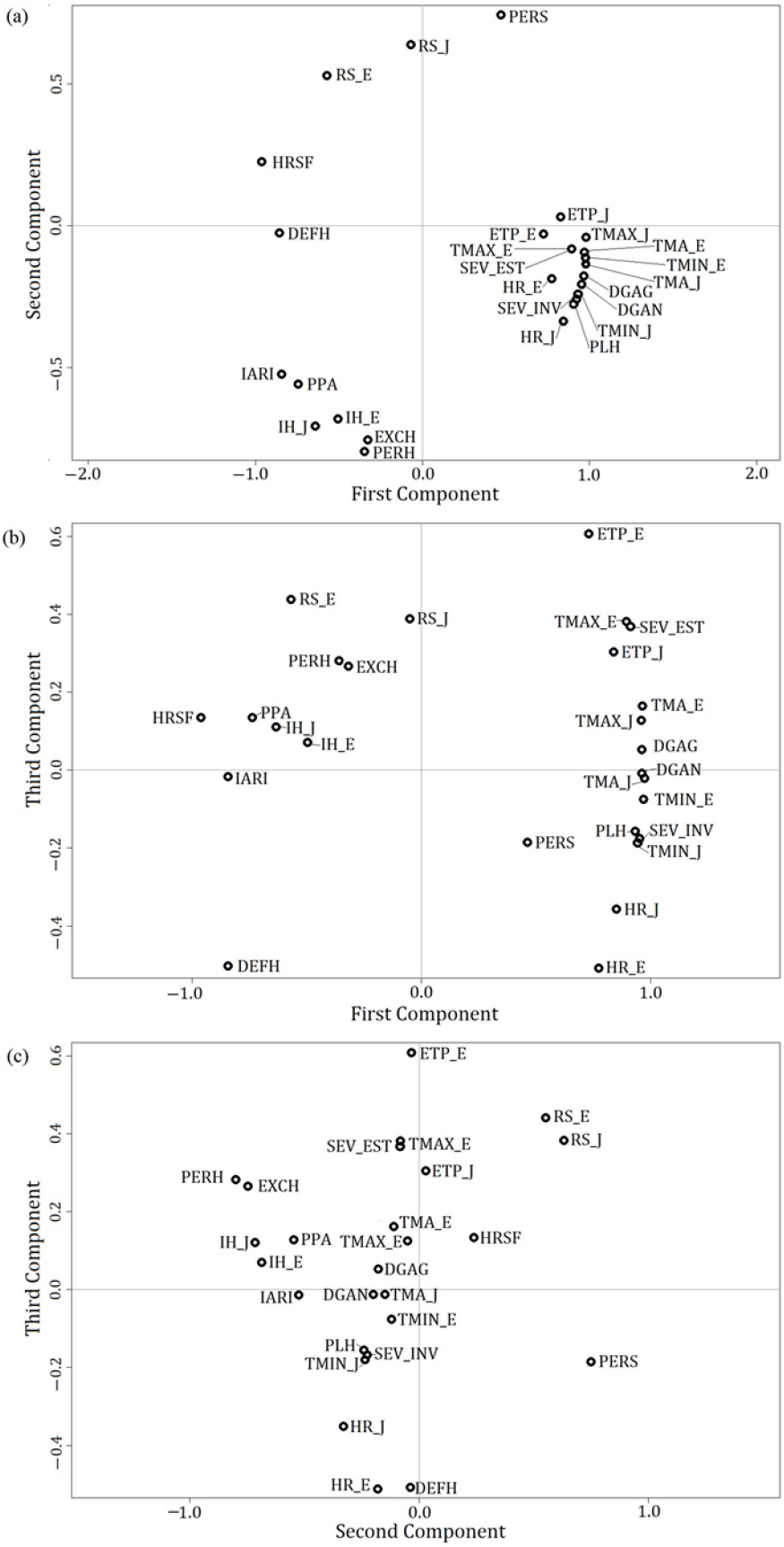

Figure 3. Correlations diagram between components and climate variables of (**a**) components 1 and 2; (**b**) components 1 and 3; and (**c**) components 2 and 3.

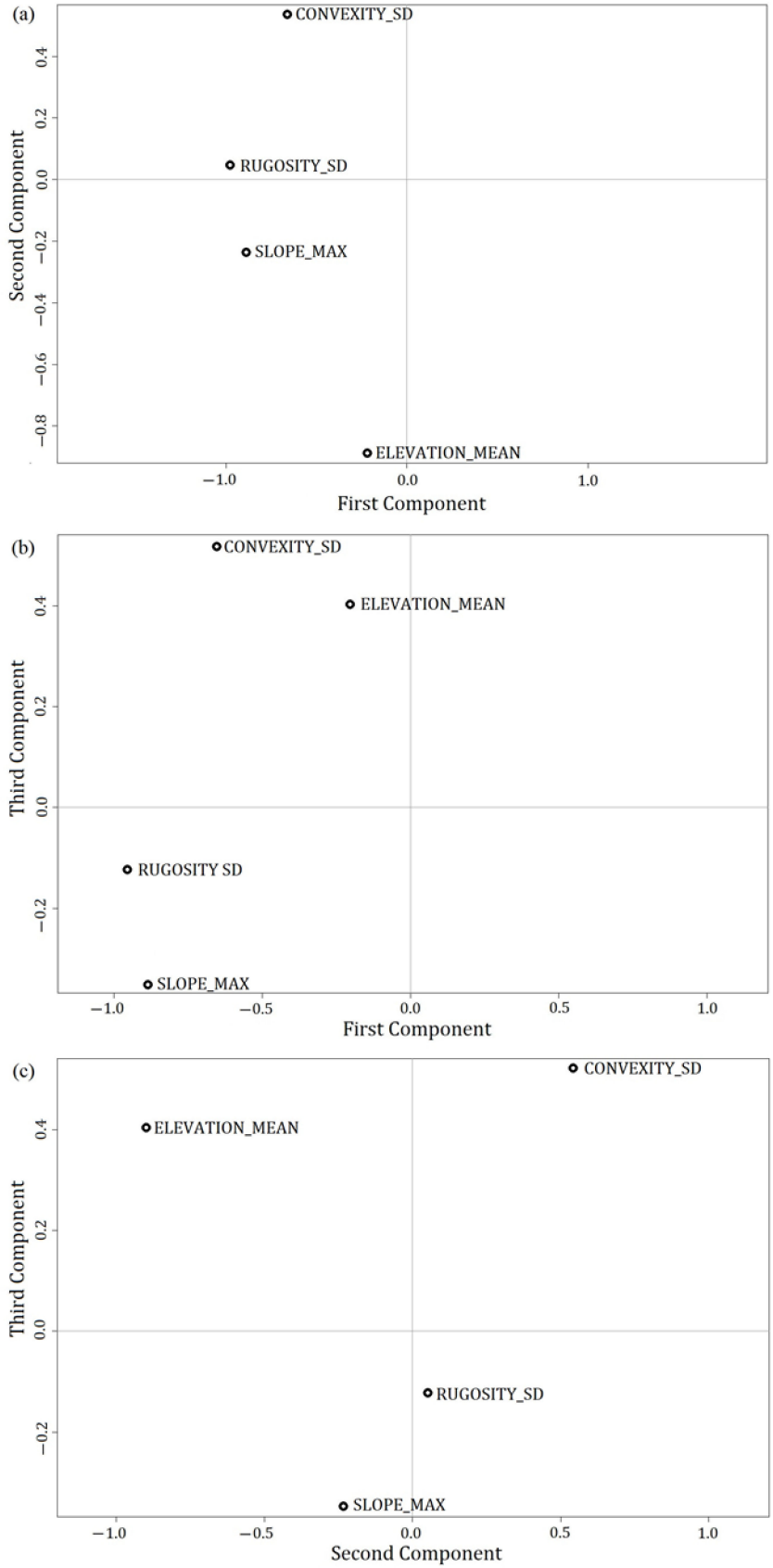

Figure 4. Correlations diagram between components and topographic variables of (**a**) components 1 and 2; (**b**) components 1 and 3; and (**c**) components 2 and 3.

Table 3. Statistical summary of four principal components obtained in the analysis for 26 climatic variables of the Atlas Bioclimático de Chile (Uribe et al. 2012) [3].

Principal Component	Standard Deviation	Explained Variance	Explained Variance (%)	Accumulated Explained Variance (%)
Climatic variables				
PC1	4.09750	16.78951	64.570	64.570
PC2	2.11840	4.48762	17.260	81.830
PC3	1.45317	2.11170	8.122	89.956
PC4	0.91295	0.83348	3.206	93.162
Topographic variables				
PC1	1.48500	2.20523	55.130	55.130
PC2	1.06820	1.14105	28.530	83.660
PC3	0.75670	0.57259	14.310	97.970
PC4	0.28505	0.08125	2.031	100.000

This climatic and topographic variable rotation improved the loadings distribution of the third component for both variables. The climatic variables resulted in loadings greater than 0.6 in the third component for the following variables: DGAG, DGAN, HR_E, HR_J, HRSF, PLH, RS_E, SEV_INV, TMA_J, TMIN_E, and TMIN_J. The topographic variable rotation resulted in loadings greater than 0.8 for each variable. The number of climatic variables with loadings greater than 0.6 in more than one component increased from one to five in the variables DGAG, DGAN, HRSF, TMA_E, and TMIN_E. Furthermore, we observed that the climatic variables DEFH, ETP_E, SEV_EST, and TMAX_E predominantly contributed to the first component, followed by IH_E, _IH_J, and PERS to the second component, and HR_E, HR_J, and RS_E to the third component. In the topographic variables, the rugosity and slope predominantly contributed to the first component, elevation to the second component, and convexity to the third component.

The climatic component number selection was validated using a residual analysis, where 10.4% of the data showed residual values greater than 0.05. The topographic residual analysis determined that there were no residuals greater than 0.05 when considering all three components.

3.1.2. CA

Twenty clusters were identified for climatic zoning (Figure 5a). It was possible to visualize different elements that characterize the region. A coastal strip is identified and, furthermore, interior zones that have a coastal influence were differentiated; the interior valleys are also delimited, especially the Copiapó and Huasco valleys (Figure 1), the climates of the premountain valleys, and the climates of mountain range and high plateau zone, where there is a variability of precipitation phenomena, due to a latitudinal effect and evapotranspiration processes that respond to elevation and solar radiation incidence. The climate zoning mapping generated with 20 groups makes climate behavior visible, integrating the climatic variability and local topographic conditions, which are shown by the patterns of agricultural use of soils and the presence of native vegetation typical of the area.

For the topographic zoning, six clusters were identified (Figure 5b), which make it possible to observe the main relief formations. This zoning shows that the Farellon (the coastal cliff of northern Chile) becomes less pronounced, and the coastal plains begin to express themselves, which constitute one of the main macro-forms in the country. In addition, it is possible to differentiate the area of transverse valleys from the Pampa area, these are relevant because they enclose the Copiapó and Huasco valleys. Finally, towards the east of the region, zoning is more precise, which is important, since the last saline basins of the region and premountain range valleys are present in this sector. The latter works as a natural climatic barrier by representing the natural boundary between the desert sector and the Los Andes mountains. It is also worth noting that, in this sector, there are mountain

ranges and foothills that, at the same time, present differences of up to 2000 m with the highest points in the region (e.g., Nevado Ojos del Salado).

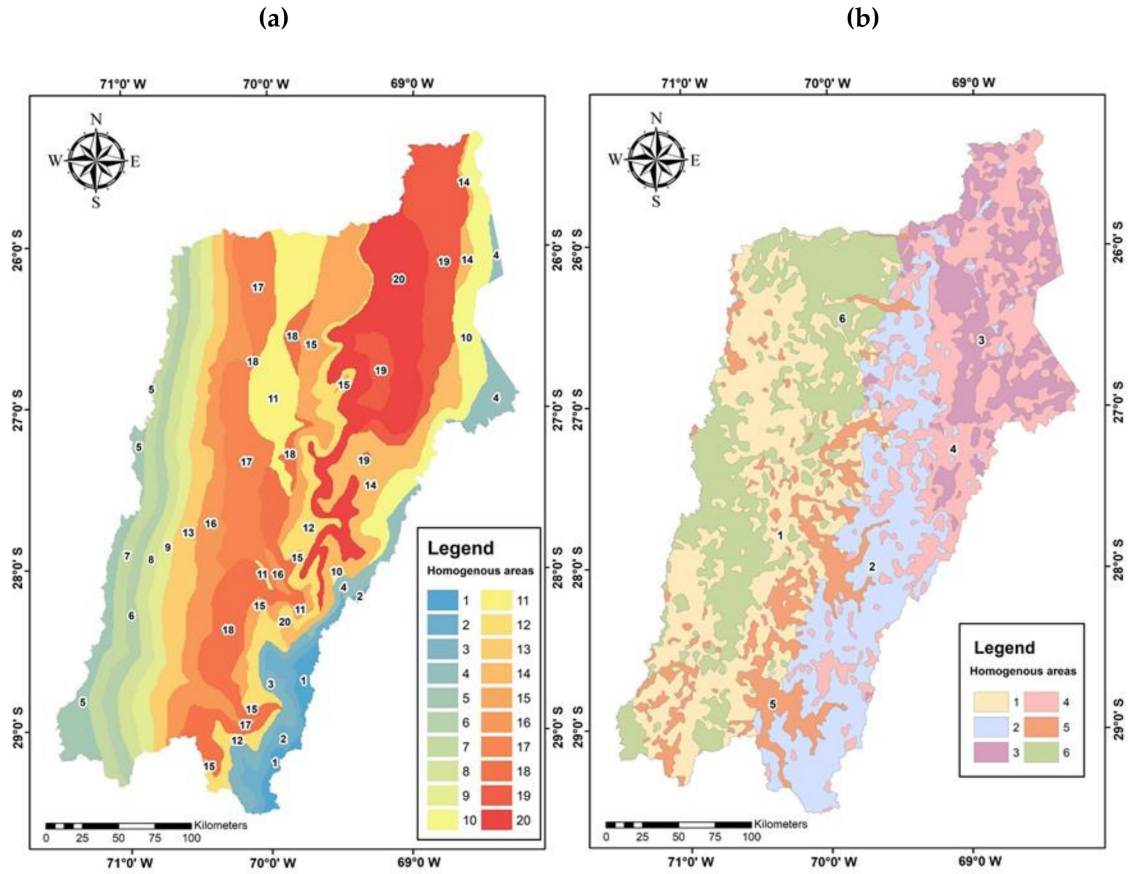

Figure 5. Zoning cartography for (**a**) climate, using 20 clusters, and (**b**) topography, using six clusters, for the Atacama region, obtained through principal component analysis (PCA) and cluster analysis (CA).

3.2. Topoclimatic Zoning

Based on the combination of climatic (Figure 5a) and topographic (Figure 5b) cartography, 61 topoclimates were obtained in the Atacama region (Figure 6a). The highest topoclimatic variability was observed in the inside zone (IZ; Figure 6b) of the region, while the coastal (CZ and IZC), northern inside zone (IZ), and mountain range zone (MZ) showed lower topoclimatic variability.

Thirteen of the 61 homogeneous areas (21.3%) in the Atacama region have surfaces of less than 386.2 km^2, while two homogeneous areas (24 and 3) comprise 3.3% of the regional surface, with areas of 3535.7 and 3546.3 km^2, respectively (Table 4). This difference in area size is mainly due to the influence that the topography has on the climate. The larger homogeneous areas are located in zones where topographic variations are small and, therefore, have similar climates, while smaller homogeneous areas indicate unique climatic regions, because their topography is different from that of their surroundings in a specific area.

Table 4. Topoclimate characterization of every homogeneous area obtained, beginning with the topoclimate zoning of the Atacama region, where TMAX_E is maximum temperatures in January (°C), TMIN_J is Minimum temperatures in July (°C), PLH is the Frost free period (days), ETP_E Evapotranspiration in January (mm month^{-1}), ETP_J Evapotranspiration in July (mm month^{-1}) and DEFH Water deficit (mm). The indicated macrozones are: MZ, mountain range zone; PV, pre-mountain range valley; HPV, high pre-mountain range valley, IPV, pre-mountain range with inside influence; IZ, inside zone; IZC, inside zone with coastal influence; and CZ, coastal zone.

Homogeneus Area	Macrozone	Area (km^2)	Altitude (m)	TMAX_E	TMIN_J	PLH	ETP_E	ETP_J	DEFH
1	MZ	2325.6	4770.6	13.5	0.0	0.0	54.2	29.7	−436.4
2	MZ	1967.4	4180.7	16.2	2.2	0.0	64.7	37.3	−574.5
3	MZ	3546.3	4348.7	16.3	2.3	0.0	65.3	38.0	−577.6
4	MZ	2308.0	4315.3	16.8	1.6	0.0	70.4	35.7	−576.5
5	MZ	832.7	4412.7	15.7	0.9	0.0	64.4	35.3	−530.3
6	PV	413.1	3973.4	17.8	3.2	0.0	72.5	37.1	−615.4
7	MZ	1470.2	4514.7	13.1	−0.1	0.0	52.1	29.2	−420.4
8	PV	2464.3	3727.9	18.4	4.1	3.1	74.3	50.3	−712.5
9	HPV	1304.3	3820.3	18.2	2.4	0.0	77.2	39.5	−647.3
10	MZ	218.4	4543.8	15.1	−0.1	0.0	63.1	30.7	−495.9
11	PV	2546.7	3843.1	19.0	4.1	8.9	78.9	45.7	−711.1
12	MZ	642.2	4748.0	10.6	−1.2	0.0	42.0	25.1	−316.4
13	IPV	366.3	2796.8	24.7	8.4	166.9	115.7	53.9	−980.3
14	IPV	540.2	2979.5	24.9	7.7	143.0	120.8	52.4	−991.2
15	PV	443.3	3339.3	23.7	5.3	69.2	115.4	46.6	−906.7
16	MZ	1028.1	4930.8	11.5	−1.3	0.0	47.2	26.2	−354.7
17	PV	2742.1	3472.1	20.1	3.9	7.5	88.2	44.7	−755.6
18	IZ	2192.7	605.2	27.8	12.6	350.5	135.0	79.3	−1261.0
19	IZ	960.7	797.9	28.4	12.3	332.8	143.3	80.8	−1319.8
20	IZ	2995.7	1572.1	28.4	10.6	233.0	150.6	65.7	−1253.3
21	IZ	2987.0	1122.4	28.5	11.7	298.7	147.9	69.9	−1263.8
22	IZ	2304.8	1049.3	28.9	11.6	278.1	152.6	81.4	−1376.8
23	IPV	1766.5	2855.3	25.6	6.5	95.0	131.4	51.0	−1030.0
24	PV	3535.7	3095.7	24.0	5.1	45.1	119.1	48.1	−938.3
25	IZC	1414.2	514.2	26.9	13.1	356.7	121.2	75.1	−1160.4
26	IZ	2010.8	832.2	27.7	12.5	341.0	133.2	76.6	−1236.9
27	IZ	2390.9	1240.0	29.4	11.9	274.2	159.3	74.5	−1359.3
28	IZ	386.1	1660.3	28.3	10.4	221.2	149.5	62.9	−1221.5
29	IPV	594.5	2308.4	25.7	7.8	150.7	128.5	54.7	−1049.3
30	IZ	649.3	1741.3	28.7	10.6	229.0	155.2	64.7	−1266.6
31	IPV	711.7	2227.8	26.1	9.6	201.3	126.7	57.4	−1065.1
32	IZC	1216.1	408.7	26.0	13.8	364.7	107.5	69.2	−1049.4
33	IZC	1603.6	676.5	26.0	13.0	363.2	111.3	63.4	−1028.5
34	CZ	1835.5	637.6	25.2	13.4	365.0	100.8	54.7	−911.5
35	IZC	1815.2	719.2	26.7	12.8	353.9	120.9	72.1	−1139.9
36	CZ	576.8	657.4	24.4	13.4	365.0	92.0	47.0	−807.4
37	CZ	1424.2	528.2	24.3	13.6	365.0	90.2	49.6	−816.2
38	IZ	667.9	2317.2	25.8	8.7	177.4	127.2	56.5	−1056.8
39	CZ	578.4	244.8	24.7	14.7	365.0	89.4	61.9	−904.9
40	CZ	1076.5	178.9	24.0	15.2	365.0	79.3	49.3	−763.4
41	CZ	364.4	776.5	25.2	12.7	365.0	104.2	52.3	−911.7
42	IZ	324.1	1730.5	27.5	10.4	227.9	139.9	59.4	−1146.0
43	IZ	2757.0	2030.9	28.1	9.7	220.7	150.0	54.1	−1149.1
44	IZ	1811.8	1945.2	28.4	9.8	218.5	153.6	55.2	−1181.2
45	PV	309.6	2434.2	24.8	5.9	69.4	125.1	49.9	−974.5
46	IZC	50.9	892.9	26.3	13.4	356.8	113.2	78.1	−1145.8
47	IZC	241.1	1049.6	26.3	12.1	364.5	118.9	55.4	−1009.2
48	IZ	104.1	766.2	28.3	13.0	360.5	139.6	71.0	−1228.4
49	IZ	1035.3	1523.8	28.7	11.7	315.3	150.3	56.0	−1171.9
50	CZ	886.5	358.1	23.8	13.6	365.0	85.7	48.0	−771.6
51	IZ	762.3	1315.9	30.0	12.3	297.3	164.8	64.7	−1312.5
52	CZ	1070.3	142.1	23.7	14.6	365.0	79.3	42.9	−700.1
53	IZ	672.5	2781.4	27.4	8.3	181.5	146.3	53.1	−1117.4
54	CZ	215.5	419.1	23.8	13.6	365.0	85.6	47.0	−760.8
55	MZ	640.7	4564.0	17.2	−0.4	0.0	76.9	26.1	−491.9
56	HPV	1117.7	4175.5	18.8	0.6	0.0	86.7	32.6	−590.0
57	HPV	286.5	4080.2	19.1	1.0	0.0	88.0	34.2	−605.0
58	PV	1349.3	3687.5	21.8	2.6	1.2	105.9	42.8	−775.5
59	PV	124.5	3935.8	21.4	1.6	0.0	104.7	39.3	−751.9
60	MZ	207.4	4751.2	15.9	−1.0	0.0	69.7	24.4	−446.1
61	MZ	465.2	4360.2	14.6	−0.2	0.0	60.6	32.1	−467.1

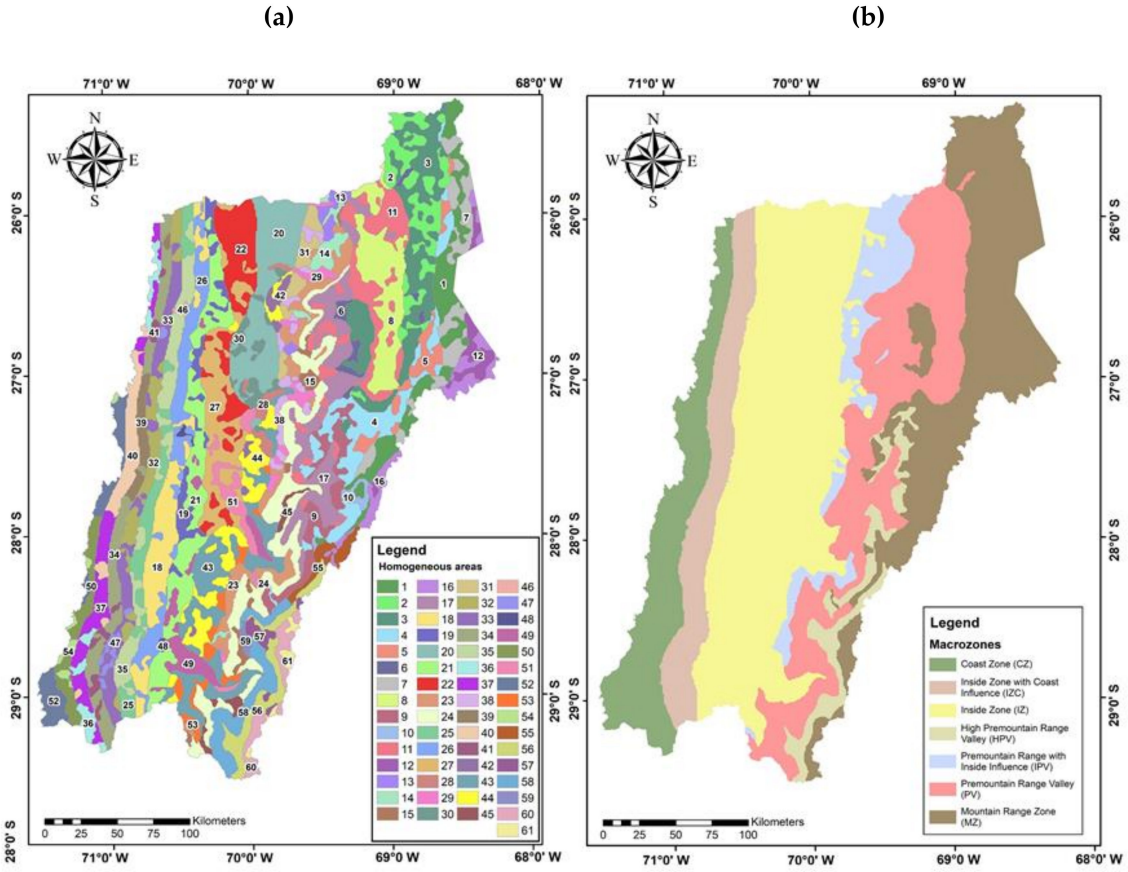

Figure 6. (**a**) Cartography of topoclimatic zoning from a combination of climatic and topographic cartographies. (**b**) Macrozones of the Atacama region that were used to characterize the topoclimates.

The identified topoclimates in the Atacama Region show a moderate thermal regime in the coast zone (CZ), without frost, and a hydrological regime with a high water deficit of approximately 700 mm year^{-1}. This condition intensifies toward the inside zone (IZ) homogeneous areas, reaching an average water deficit of 1200 mm year^{-1}, and higher annual thermal amplitude (over 24 °C). The inside zone with coastal influence (IZC) and pre-mountain range with inside influence (IPV) topoclimates show reduced temperatures that influence their thermal regime and moderate their water deficit. The high pre-mountain range valleys (HPV) and mountain range zone (MZ) exhibited diminishing temperatures with increasing altitude, a more significant frost regime, and minor regional hydrological deficits due to a lower evapotranspiration rate (Figure 6a,b; Table 4).

3.3. Regional AWS Representation Area

There are 16 AWSs installed in the Atacama region (Table 2), which cover 2364.7 km^2 (3.1% of the regional surface area). Topoclimatic overrepresentation (refers to the presence of more than one AWS in a homogenous topoclimate area in which all stations obtain meteorological information in a similar manner) was identified in homogeneous area 25, where there are three AWSs. In area 49, there are five AWSs, while in area 51, there are two AWSs (Figure 7). Moreover, we identified AWSs established along the borders of the homogeneous areas. In homogeneous area 49, there are four AWSs located along the border, which are adjoined to homogenous areas 51 and 43. Homogeneous areas 25 and 26 have one AWS adjoined to areas 32 and 18, respectively. Therefore, the homogeneous areas indirectly represented by an AWS comprise an area of 8725.4 km^2. Those not represented by an AWS comprise an area greater than 64,560.8 km^2.

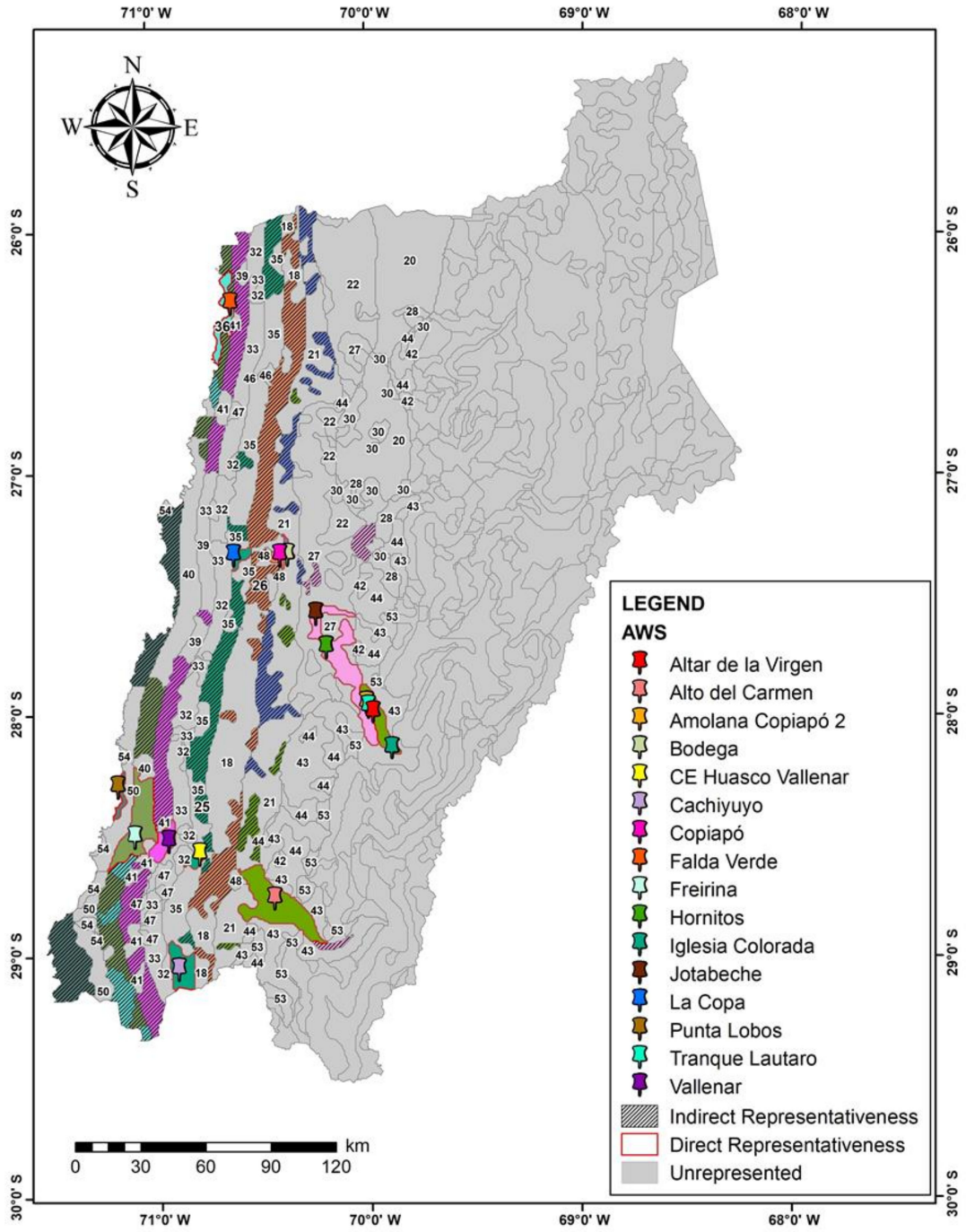

Figure 7. Cartography of automatic weather station (AWS) topoclimatic representativeness and that of adjacent areas.

4. Discussion

4.1. PCA and CA Methodology for Topoclimatic Zoning

The PCA and CA methodology applied to climatic and topographic information layers to identify homogeneous areas in the Atacama region showed satisfactory results for the study, since consistent zoning was obtained with the characteristics and particularities of the region in terms of climate and topography, managing to reflect the complexity of the territory.

PCA and CA have been widely used for information reduction and subsequent grouping in different areas, such as biology, psychology, and other disciplines, but their application in atmospheric

sciences was less known [77]. However, this has changed over time, and the numerical grouping methodology of climatic variables was found to be an efficient way of detecting homogeneous climatic areas in relatively small regions [78–80].

One of the difficulties presented by the method is the instability in the conformation of the established clusters, which is due to the randomness of the K-means method [81,82]. This can be addressed by executing the K-means algorithm several times (10 times in this study) to reduce the probability of obtaining a low-quality solution. Other techniques previously used to evaluate the cluster stability involve the repetition of the grouping process by selecting different centroids, where the best solution is that defined by clusters with the greatest difference between them [83]. Brewer et al. (2007) [84] determined cluster stability by repeating data grouping several times with different initial centroids, verifying graphically that the groups remain stable. This added a strong subjectivity component [69]. Brewer et al. (2007) [85] performed 1000 iterations and estimated the standard deviation of the centroid attribution value. Low values (lower than 19.71) indicate that the centroids did not change significantly and a stable solution. Mahlstein and Knutti (2010) [86] compared the ten best solutions, which were selected based on the sum of the standard deviations within a group from the K-means method. The standard deviations were similar to the selected solutions because the resulting regions had clearly defined parameters. Mahlstein and Knutti (2010) [86] evaluated the similarity between the solutions, according to their correlations. Methodologies applied by Brewer et al. (2007) [84], Brewer et al. (2007) [85], and Mahlstein and Knutti (2010) [86] provided greater certainty with respect to conglomerate stability, but their assessment required more analyses, which complicated the procedure. For this reason, we applied a simpler method in this study.

4.2. Climatic and Topographic Cartography of the Atacama

The results obtained in the climatic and topographic cartographies were consistent with registered conditions in the Atacama region [9,13,39,45,87]. Juliá et al. (2008) [13] used the Köppen classification to describe the Atacama regional climate by identifying four climate types: coastal desert with abundant cloudiness (BWn), transitional desert weather (BWi), mountainous cold desert weather (BWk'G), and high-mountain tundra weather (EB). Similar to this study, the climate distribution has a longitudinal behavior, because it changes as it moves away from the coast, as well as with increasing altitude. Nevertheless, these climatic divisions were different, given the level of detail reported in each study, due to the working scale. Juliá et al. (2008) [13] used the Köppen classification, which is a zoning method carried out globally with basic temperature and precipitation variables, applying it on a regional scale, while this study was developed on a local scale. Sarricolea et al. (2017) [39] updated the Köppen climatic cartography in Chile, where the climate distribution did not present a longitudinal structure as determined in this study. Although Sarricolea et al. (2017) [39] indicate that the obtained climate zoning in the Chilean "*Norte Chico*" resembled less than 40% of the data from meteorological stations (used for comparisons), the divisions among the various climates did not resemble those obtained in this study.

In the inside zone of the Atacama region, near the Los Andes mountains, we identified a climatic convexity in the Copiapó and Huasco rivers (Figure 5a). Uribe et al. (2012) [3] also determined that this convexity, corresponding to the valleys surrounded by mountainous cords, is relevant because it represents that the topography influences unique climatic regions. Unlike this study, Uribe et al. (2012) [3] established the presence of three districts in the coastal zone, which define a homogeneous zone along the coast. This difference may be due to the fact that the climatic zones reported in Uribe et al. (2012) [3] were obtained by crossing the climatic layers, whereas in this study, we used the CA methodology.

The topographic zoning of the Atacama region (Figure 5b) described here maintained similar patterns to those reported in Novoa et al. (2008) [9]. However, Novoa et al. (2008) [9] defined regions of austral undulating Pampas, transitional Pampas, and fluviomarine plains, which were not observable in the current topographic zoning results. This may be due to the fact that, in this study, the cartographs

were generated based on topographic parameters extracted from a DEM, which did not consider original relief formations. Hence, each zone, whose evaluated parameters were similar, was identified as a unique entity.

4.3. Topoclimatic Cartography of the Atacama Region

A topoclimate can be described according to geographical units, which, once the units are sectored, should contain homogeneous gradients of climate variation [1]. The topography used to identify homogeneous climate areas, as well as the climate variables, was evenly distributed and began at a specific point [3,37,38]. In this study, the PCA and CA were independently applied to the climatic and topographic variables. Based on this combined approach, we identified areas with similar topoclimatologies.

The results of this study differed from those obtained by Santibáñez et al. (2017) [38] in the Atlas Agroclimático de Chile, which identified 23 homogeneous units in the Atacama region. In this study, our analyses established 61 homogeneous areas (Figure 6a). This difference between these results may be due the level of detail in the generated cartographs, as well as the use of a specific method. The CA was used in both studies but was applied in different ways. In this study, it was applied separately to the climatic and topographic variables, while in the Atlas Agroclimático de Chile, it was applied to a set of climatic layers (i.e., temperature, precipitation, humidity, and solar radiation) that were included in their model of the topographic parameters of latitude, altitude, distance to the sea, and local topographic factors. For this reason, in our study, more detailed and fragmented homogeneous areas were obtained. In this study, even if the climatic conditions in an area persist, if the topographic unit changed, the homogeneous area was classified as a different climate. The analysis performed in this study should be understood in the context of the integration of spatial (geographical) factors, and their incidence in the expression of the behavior of a particular climatic variable. The concept of topoclimate allows us to address this complexity by integrating the variability in the climatic parameters of the thermal (TMAX_E, TMIN_J, and PLH) and hydric (ETP_E, ETP_J, and DEFH) regime with the local topography conditions and spatial conformation of the study area.

Both studies (Santibáñez et al. (2017) [38] and this study) conform to the objectives for which they were performed, i.e., establishing agroclimatic districts and estimating the representative area of an AWS, respectively. The developed zoning scale determines their applicability for different matters (in this study, a local scale). This difference in scale explains the variation in the homogeneous-area identifications. In addition, in this study, the topographic variables that characterize the topography were given a major weight, which is based on the topoclimate concept. This factor also influences the representative area of an AWS.

This study intends to establish a methodology that can be replicated for the identification of the representative area of an AWS, as it can be applied to other previously processed studies that contain layers of climatic information, which renders this methodology simple and rapid.

The current topoclimate zoning proposal for the Atacama region (Figure 6a,b) exhibits a spatial structure that represents its particular geography, integrating singular topoclimate phenomena. This proposal determines the closeness of the coast and its influence, the altitudinal tier distribution, the transverse valley conformation, and a solar radiation latitudinal expression. The solar radiation latitudinal expression is determined using an isothermic distribution, with a noticeable increase toward the inner valleys and decrease along the coast and foothill zones. Altitudinal tiers of the foothills and mountain ranges exhibit colder and more extreme topoclimates.

4.4. Representative Area of the AWSs Installed in the Atacama Region

The identification of representative areas of the AWSs based on the delineation of the topoclimatic zones used the features of each homogenous area that mainly depend on the type of climate and topography in the study area [88–90]. Therefore, each homogenous area had a climate with similar behaviors, whose details were added to the topography that determined the collected climate

information. The AWS location within a homogeneous area was related to the spatial resolution of the study area, as this will depend on the location of each AWS, especially for those located at the limits of the homogenous area (e.g., in this study, four stations located along the edge of homogenous area 49 were registered, as shown in Figure 7). The validation of every representative area must be accomplished using meteorological data and measured at an AWS within each area to ensure its accurate representation. The fact that each climatic variable can have a singular behavior indicates that we must also consider that each has a particular representative area [8].

Caroca et al. (2015) [10] estimated the influencing areas for meteorological stations in the National Agroclimatic Network (*Red Agroclimática Nacional* (RAN)) by comparing the spatial climate variables for the territory with the same variables in the AWS region, which established a maximum similarity limit between these values within a 50 km radius. Their study considered nine AWSs, while this study used 16. Representative areas matched the independent direct homogeneous identification for every station, including area 51, which, according to their study, is shared by the Hornitos and Jotabeche stations. Meanwhile, the Amolana Copiapó and Tranque Lautaro stations have the same representation area in both studies (Figure 7).

The surface of every homogeneous area was different in each case. Caroca et al. (2015) [10] defined larger representative areas than in this study, except for areas 28 (49 in our study) and 24 (51 in this study), whose extent was reduced by 52.3 and 410.3 km^2, respectively. Area 27 (25 in this study) exhibited a greater size may, which was 1583.4 km^2 more in their study. This discrepancy could result from using topographic variables that aim to characterize, in detail, the surface, reducing representation and defining areas that are more spatially discontinuous. In addition, Caroca et al. (2015) [10] used the climatic layers from the Atlas Agroclimático de Chile [38]. This was performed to define the agroclimatic districts, which is different from this study, where the topoclimatic zoning was developed to define representative areas.

We observed that AWS installations in the region generally do not follow the parameters related to spatial representativeness. The AWSs are not installed in homogenous topoclimatic units, as the prevailing criteria for an AWS location are determined according to the interests of the installing entity. Other applications that may provide meteorological information on topics of relevance to the region, such as the management of water resources, the conservation of endemic flora and fauna, and natural disaster occurrences, have not been considered a priority in terms of AWS installation.

Accounting for the importance of meteorological information in different areas, 61 AWSs should be available to represent the topoclimatic variability of this region, approximately twice the number suggested by WMO for a mountainous area with the surface area of the Atacama region (30 AWS) [17], which indicates the importance of integrating topographic parameters in this type of study. Due to the abrupt topography of the region, the WMO criterion that requires a rain gauge every 2500 km^2 [17] is not applicable.

Estimation of the representative areas can be used for optimal zone planning and new AWS placements, which can help to increase network density. However, given that resources for AWS installations are limited, the possible topoclimates where new AWSs may be located should be selected based on establishing prioritization criteria according to the productive, environmental, or social purposes for which they are required. An increase in AWS density could improve the quality of the climate and meteorological information currently available in the region, which is also relevant in a context of climate change [91] and the effects that it could generate in the economic activities carried out in the Atacama region.

5. Conclusions

Topoclimatic zoning of the Atacama region established the presence of 61 topoclimatic homogenous areas, which can be considered as equivalent to the AWS representative areas in the Atacama region.

Only 3.1% of the Atacama region's surface area is directly represented by an AWS, while 11.5% is represented indirectly. On the other hand, the regional surface area without AWS representation is

85.3%, indicating a lack of AWS coverage in the region, and the need to expand climatic information coverage. Homogeneous areas with AWS overrepresentation were also registered, indicating the lack of planning with respect to their installation.

The methodology used in this study to identify topoclimatic zones can be replicated in other regions of the world, to provide more detailed climate information than is currently available. This methodology can also be used in the planning and installation of AWSs, both in the Atacama region and at the national level, facilitating an integrated network that allows for wider coverage for future climate studies in Chile. Using other statistical support methods and advanced techniques to validate the conglomerate stability may also improve this approach.

The results for AWS representative areas can also be used to understand the behavior of areas with similar climates, where AWSs are not currently available. This can help the current understanding of different natural phenomena and is useful for planning activities in the region.

6. Software

Maps were created using ESRI ArcGIS 10.4 software and the climate surfaces provided in Uribe et al. (2012) [3]. Statistical procedures were performed using the R-Studio 3.4.3 software.

Supplementary Materials: The following are available online at http://www.mdpi.com/2073-4433/11/6/611/s1.

Author Contributions: Conceptualization, D.C. and M.P.; Formal analysis, D.C., R.P., S.H. and J.M.U.; Investigation, D.C., R.P., S.H. and J.M.U.; Methodology, D.C., R.P., S.H., J.M.U. and M.P.; Resources, M.P.; Supervision, M.P.; Validation, J.M.U.; Visualization, D.C., R.P. and S.H.; Writing—Original draft, D.C.; Writing—Review & editing, M.P. All authors have read and agreed to the published version of the manuscript.

Funding: This work was funded by Agroenergía Ingeniería Genética S.A.

Conflicts of Interest: The authors have no conflicts of interest to declare.

References

1. Ferrer, F.; Cabrera, P.; García, P.; de Nicolás, J. Metodología sobre cartografía bioclimática. In *Clima y Agua: La Gestión de un Recurso Climático*; Dorta, P., Valladares, P., Eds.; Tabapress: Tenerife, Spain, 1996; pp. 365–378.
2. OMM (Organización Meteorológica Mundial). *Documento Técnico N° 100*; Organización Meteorológica Mundial: Ginebra, Suiza, 2011.
3. Uribe, J.M.; Cabrera, R.; de la Fuente, A.; Paneque, M. *Atlas bioclimático de Chile*; Universidad de Chile: Santiago, Chile, 2012.
4. Meza, F.; Pszczólkowski, P.; Kosiel, K. Modelación topoclimática: Descubrir el terroir vitícola. *Rev. Agron. For. UC* **2006**, *30*, 22–25.
5. Azorin-Molina, C.; Asin, J.; McVicar, T.R.; Minola, L.; Lopez-Moreno, J.L.; Vicente-Serrano, S.M.; Chen, D. Evaluating anemometer drift: A statistical approach to correct biases in wind speed measurement. *Atmos. Res.* **2018**, *203*, 175–188. [CrossRef]
6. Yang, W.; Guo, X.; Wang, Y. Observational evidence of the combined influence of atmospheric circulations and local factors on near-surface meteorology in Dagze Co basin, inner Tibetan Plateau. *Int. J. Climatol.* **2018**, *38*, 2056–2066. [CrossRef]
7. López, J. Propuesta metodológica para el rediseño de una red meteorológica en un sector de la región Andina Colombiana. *Publ. Investig.* **2014**, *8*, 55–76. [CrossRef]
8. WMO (World Meteorological Organization). *Instruments and Observing Methods (Doc, Tec. N° 589)*; World Meteorological Organization: Geneva, Switzerland, 1993.
9. Novoa, J.; Tracol, Y.; López, D. Paisajes eco-geográficos de la región de Atacama. In *Libro Rojo de la Flora Nativa y de Los Sitios Prioritarios Para su Conservación*; Squeo, F., Arancio, G., Gutiérrez, J.R., Eds.; Ediciones Universidad de La Serena: La Serena, Chile, 2008; pp. 13–24.
10. Caroca, C.; Santibáñez, P.; Santibáñez, F.; Ruiz, R.; Campos, C.; Bravo, R. *Estudio de la Cobertura Actual y Futura de la Red Agroclimática Nacional. Serie de Estudios para la Innovación FIA*; Fundación para la Innovación Agraria: Santiago, Chile, 2015.

11. Romero, H.; Vinagre, J. Topoclimatología de la cuenca del Río Mapocho. *Investig. Geográficas* **1985**, 3–30. [CrossRef]
12. Antonioletti, R.; Schneider, H.; Borcosque, J.L.; Zarate, E. *Características climáticas del Norte Chico (26° a 33° latitud sur)*; Instituto de Investigación de Recursos Naturales: Santiago, Chile, 1972.
13. Juliá, C.; Montecinos, S.; Maldonado, A. Características climáticas de la región de Atacama. In *Libro rojo de la Flora Nativa y de los Sitios Prioritarios Para su Conservación: Región de Atacama*; Squeo, F., Arancio, G., Gutiérrez, J.R., Eds.; Ediciones Universidad de La Serena: La Serena, Chile, 2008; pp. 25–42.
14. Gómez, F.; Afonso, A. The Social Capital, Institutions and Economic Development: The revisited experience of EMPRENDE Chile. In *Planning and Community Development: Case Studies*; Migdely, J., Cazorla, A., Eds.; ETSI Agrónomos: Madrid, Spain, 2012; pp. 249–284.
15. Agroclima. Available online: www.agroclima.cl (accessed on 15 April 2020).
16. INE (Instituto Nacional de Estadística). *División Político Administrativa y Censal*; Región de Atacama, Ministerio de Economía, Fomento y Turismo: Santiago, Chile, 2007.
17. WMO (World Meteorological Organization). *Guide to Hidrological Practices (Doc, Tec. N° 168)*; World Meteorological Organization: Geneva, Switzerland, 2008.
18. Milewska, E.; Hogg, W.D. Spatial representativeness of a long-term climate network in Canada. *Atmos Ocean.* **2001**, *39*, 145–161. [CrossRef]
19. Orlowsky, B.; Seneviratne, S.I. On the spatial representativeness of temporal dynamics at European weather stations. *Int. J. Climatol.* **2014**, *34*, 3154–3160. [CrossRef]
20. Köppen, W. *Climatología*; Fondo de Cultura Económica: Mexico City, México, 1948.
21. Thornthwaite, C.W. An approach toward a rational classification of climate. *Geogr. Rev.* **1948**, *38*, 55–94. [CrossRef]
22. Bagnouls, F.; Gaussen, H. Les climats biologiques et leur classification. *Ann. Georgr.* **1957**, *66*, 193–220. [CrossRef]
23. Bunkers, M.J.; Miller, J.R.; DeGaetano, A.T. Definition of climate regions in the Northern Plains using an objective cluster modification technique. *J. Clim.* **1996**, *9*, 130–146. [CrossRef]
24. DeGaetano, A.T. Delineation of mesoscale climate zones in the Northeastern United States using a novel approach to cluster analysis. *J. Clim.* **1996**, *9*, 1765–1782. [CrossRef]
25. Unal, Y.; Kindap, T.; Karaca, M. Redefining the climate zones of Turkey using cluster analysis. *Inter. J. Climatol.* **2003**, *23*, 1045–1055. [CrossRef]
26. Kottek, M.; Grieser, J.; Beck, C.; Rudolf, B.; Rubel, F. World map of the Köppen-Geiger climate classification updated. *Meteorol. Z.* **2006**, *15*, 259–263. [CrossRef]
27. Peel, M.C.; Finlayson, B.L.; Mcmahon, T.A. Updated world map of the Köppen-Geiger climate classification. *Hydrol. Earth Syst. Sci.* **2007**, *11*, 1633–1644. [CrossRef]
28. Rubel, F.; Kottek, M. Observed and projected climate shifts 1901–2100 depicted by world maps of the Köppen-Geiger climate classification. *Meteorol. Z.* **2010**, *19*, 135–141. [CrossRef]
29. Yunus, F.; Shafie, A.; Jaafar, J.; Mahmud, Z. Homogeneous climate divisions for Peninsular Malaysia. *Geodin. Acta.* **2011**, *24*, 89–94. [CrossRef]
30. Iyigun, C.; Türkeş, M.; Batmaz, İ.; Yozgatligil, C.; Purutçuoğlu, V.; Koç, E.K.; Öztürk, M.Z. Clustering current climate regions of Turkey by using a multivariate statistical method. *Theor. Appl. Climatol.* **2013**, *114*, 95–106. [CrossRef]
31. Vondráková, A.; Vávra, A.; Voženílek, V. Climatic regions of the Czech Republic. *J. Maps.* **2013**, *9*, 425–430. [CrossRef]
32. Belda, M.; Holtanová, E.; Halenka, T.; Kalvová, J. Climate classification revisited: From Koppen to Trewartha. *Clim Res.* **2014**, *59*, 1–13. [CrossRef]
33. Di Castri, F.; Hajek, E.R. *Bioclimatología de Chile*; Vicerrectoría Académica de la Universidad Católica de Chile: Santiago, Chile, 1976.
34. Novoa, R.; Villaseca, S.; Del Canto, P.; Rouanet, J.; Sierra, C.; Del Pozo, A. *Mapa Agroclimático de Chile*; Instituto de Investigaciones Agropecuarias: Santiago, Chile, 1989.
35. Santibáñez, F.; Uribe, J.M. *Atlas agroclimático de Chile: Regiones IV a IX*; Universidad de Chile: Santiago, Chile, 1993.
36. Amigo, J.; Ramírez, C. A bioclimatic classification of Chile: Woodland communities in the temperate zone. *Plant Ecol.* **1998**, *136*, 9–26. [CrossRef]

37. Morales, L.; Canessa, F.; Mattar, C.; Orrego, R.; Matus, F. Caracterización y zonificación edáfica y climática de la Región de Coquimbo, Chile. *Rev. Cienc. Suelo Nutr. Veg.* **2006**, *6*, 52–74.
38. Santibáñez, F.; Santibáñez, P.; Caroca, C.; González, P. *Atlas agroclimático de Chile. Tomo II: Regiones de Atacama y Coquimbo*; Universidad de Chile: Santiago, Chile, 2017.
39. Sarricolea, P.; Herrera-Ossandon, M.; Meseguer-Ruiz, Ó. Climatic regionalisation of continental Chile. *J. Maps.* **2017**, *13*, 66–73. [CrossRef]
40. Fovell, R.G.; Fovell, M.Y.C. Climate zones of the conterminous United States defined using cluster analysis. *J. Clim.* **1993**, *6*, 2103–2135. [CrossRef]
41. Sahin, S.; Cigizoglu, H.K. The effect of the relative humidity and the specific humidity on the determination of the climate regions in Turkey. *Theor. Appl. Climatol.* **2013**, *112*, 469–481. [CrossRef]
42. Sarmadi, F.; Azmi, M. Regionalizing mean air temperature in Iran by multivariate analysis and L-moment methods. *J. Hydrol. Eng.* **2016**, *21*, 05015018. [CrossRef]
43. Gómez-Zotano, J.; Alcántara-Manzanares, J.; Olmedo-Cobo, J.A.; Martínez-Ibarra, E. La sistematización del clima mediterráneo: Identificación, clasificación y caracterización climática de Andalucía (España). *Rev. Geogr. Norte Gd.* **2015**, 161–180. [CrossRef]
44. SUBDERE (Subsecretaría de Desarrollo Regional y Adinistrativo). *División Político Administrativa de Chile*; SUBDERE: Santiago, Chile, 2016.
45. Maldonado, A.; Rozas, E. Clima y paleoambientes durante el cuaternario tardío en la región de Atacama. In *Libro Rojo de la flora Nativa y de Los Sitios Prioritarios Para su Conservación: Región de Atacama*; Squeo, F., Arancio, G., Gutiérrez, J.R., Eds.; Ediciones Universidad de La Serena: La Serena, Chile, 2008; pp. 293–304.
46. Ulloa, R.; De Zárate, P.O. *Geografía III Región de Atacama. Colección Geografía de Chile*; Ediciones Instituto Geográfico Militar: Santiago, Chile, 1989.
47. Allaby, M. *Encyclopedia of Weather and Climate*; Facts on File: New York, NY, USA, 2002.
48. Google Earth Engine. Available online: https://explorer.earthengine.google.com (accessed on 15 April 2020).
49. Böhner, J.; Antonić, O. Land-surface parameters specific to topo-climatology. In *Geomorphometry: Concepts, Software, Applications*; Hengl, T., Reuter, H.I., Eds.; Elsevier: Amsterdam, The Netherlands, 2009; pp. 195–226.
50. Vicente-Serrano, S.M.; El Kenawy, A.; Azorin-Molina, C.; Chura, O.; Trujillo, F.; Aguilar, E.; Martín-Hernández, N.; López-Moreno, J.I.; Sánchez-Lorenzo, A.; Moran-Tejeda, E.; et al. Average monthly and annual climate maps for Bolivia. *J. Maps* **2016**, *12*, 295–310. [CrossRef]
51. OMM (Organización Meteorológica Mundial). *Manual del Sistema Mundial Integrado de Sistemas de Observación de la OMM*; Anexo VIII del reglamento técnico de la OMM; Organización Meteorológica Mundial: Ginebra, Suiza, 2015.
52. Felicísimo, Á.M. *Modelos Digitales del Terreno: Introducción y Aplicaciones en las Ciencias Ambientales*; Pentalfa: Oviedo, Spain, 1994.
53. Beguería, S.; Lorente, A. Distribución espacial del riesgo de precipitaciones extremas en el Pirineo aragonés occidental. *Geographicalia* **1999**, *37*, 17–36. [CrossRef]
54. Mazzoleni, S.; Porto, A.L.; Blasi, C. Multivariate analysis of climatic patterns of the Mediterranean basin. *Vegetatio* **1992**, *98*, 1–12. [CrossRef]
55. Bholowalia, P.; Kumar, A. EBK-means: A clustering technique based on elbow method and k-means in WSN. *Int. J. Comput Appl.* **2014**, *105*, 17–24.
56. Bro, R.; Smilde, A.K. Principal component analysis. *Anal. Methods* **2014**, *6*, 2812–2831. [CrossRef]
57. Kendall, M. A new measure of rank correlation. *Biometrika* **1938**, *30*, 81–93. [CrossRef]
58. Carvajal, E.Y.; Marco, S.J.B. Análisis de variabilidad de datos medioambientales aplicando funciones ortogonales empíricas o componentes principales. *Ing. Recur. Nat. Ambiente* **2004**, *1*, 4–12.
59. Pino, M.; Mulsow, S. Distribución de faces granulométricas en el estuario del Río Queule, IX región: Un análisis de componentes principales. *Rev. Geológica Chile* **2010**, *18*, 77–85.
60. Vyas, S.; Kumaranayake, L. Constructing socio-economic status indices: How to use principal components analysis. *Health Policy Plan.* **2006**, *21*, 459–468. [CrossRef] [PubMed]
61. Peña, D. *Análisis de Datos Multivariantes*; McGraw-Hill: Madrid, Spain, 2002.
62. Jolliffe, I.T. Principal component analysis and factor analysis. In *Principal Component Analysis*; Jolliffe, I.T., Ed.; Springer: New York, NY, USA, 1986; pp. 115–128.
63. Mardia, K.; Kent, J.; Bibby, J.M. *Multivariate Analysis*; Academic Press: London, UK, 1979.
64. Cattell, R.B. The scree test for the number of factors. *Multivar. Behav. Res.* **1966**, *1*, 245–276. [CrossRef]

65. Rodríguez-Jaume, M.; Mora, C.R. Análisis de varianza simple (o con un factor), factorial y multivariable. In *Estadística Informática: Casos y Ejemplos con el SPSS*; Rodríguez-Jaume, M., Mora, C.R., Eds.; Universidad de Alicante: Alicante, Spain, 2001; pp. 179–211.
66. Osborne, J.W. What is rotating in exploratory factor analysis. *Pract. Assess. Res. Eval.* **2015**, *20*, 2.
67. Lozares, C.C.; López, R.P. El análisis de componentes principales: Aplicación al análisis de datos secundarios. *Rev. Sociol.* **1991**, *37*, 31–63. [CrossRef]
68. Steiger, J.H.; Lind, J.C. *Statistically Based Tests for the Number of Common Factors*; Annual Meeting of the Psychometric Society: Iowa City, IA, USA, 1980.
69. Ferrando, P.J.; Anguiano-Carrasco, C. El análisis factorial como técnica de investigación en psicología. *Pap. Psicol.* **2010**, *31*, 18–33.
70. Núñez-Colín, C.A.; Escobedo-López, D. Uso correcto del análisis clúster en la caracterización de germoplasma vegetal. *Agron. Mesoam.* **2011**, *22*, 415–427. [CrossRef]
71. De la Fuente, S. *Análisis Conglomerados*; UAM, Facultad de Ciencias Económicas y Empresariales: Madrid, Spain, 2011.
72. Della-Nave, M.; Donadio, I. *Classificazione del Clima di Varese e Milano Mediante Cluster Analysis, Persistenza e Ariabilità*; Politecnico de Milano: Milano, Italy, 2014.
73. Hartigan, J.A.; Wong, M.A. Algorithm AS 136: A k-means clustering algorithm. *J. R. Stat. Soc. C-Appl.* **1979**, *28*, 100–108. [CrossRef]
74. Wagstaff, K.; Cardie, C.; Rogers, S.; Schrödl, S. Constrained k-means Clustering with Background Knowledge. In Proceedings of the eighteenth international conference on machine learning, ICML, Williamstown, MA, USA, 28 June–1 July 2001.
75. Kodinariya, T.M.; Makwana, P.R. Review on determining number of cluster in k-means clustering. *Int. J. Adv. Res. Comput. Sci. Manag. Stud.* **2013**, *1*, 90–95.
76. Ureña-Elizondo, F. Utilización de estaciones meteorológicas automáticas como nueva alternativa para el registro de transmisión de datos. *Rev. Electrónica Sist. Estud. Posgrado* **2011**, *11*, 33–49. [CrossRef]
77. Wolter, K. The Southern Oscillation in surface circulation and climate over the tropical Atlantic, Eastern Pacific, and Indian Oceans as captured by cluster analysis. *J. Clim. Appl. Metereol.* **1987**, *26*, 540–558. [CrossRef]
78. Rosini, E.; Menenti, M.; Trevisan, V. Concetti e metodi della mesoclimatologia per un contributo alia conoscenza ambientale. *Inf. Bot. Ital.* **1974**, *6*, 163–207.
79. Galliani, G.; Filippini, F. Climatic clusters in a small area. *Int. J. Climatol.* **1985**, *5*, 487–501. [CrossRef]
80. Hubálek, Z.; Horáková, M. Evaluation of climatic similarity between areas in biogeography. *J. Biogeogr.* **1998**, *15*, 409–418. [CrossRef]
81. Sharma, R.; Alam, M.; Rani, A. K-means clustering in spatial data mining using weka interface. In Proceedings of the International Conference on Advances in Communication and Computing Technologies (ICACACT'12), Mumbai, India, 11 August 2012; Volume 1, pp. 26–30.
82. Baswade, A.M.; Nalwade, P.S. Selection of initial centroids for k-means algorithm. *Int. J. Comput. Sci. Mob. Comput.* **2013**, *2*, 161–164.
83. Bonfils, C.; de Noblet-Ducoudré, N.; Guiot, J.; Bartlein, P. Some mechanisms of mid-Holocene climate change in Europe, inferred from comparing PMIP models to data. *Clim. Dyn.* **2004**, *23*, 79–98. [CrossRef]
84. Brewer, S.; Alleaume, S.; Guiot, J.; Nicault, A. Historical droughts in Mediterranean regions during the last 500 years: A data/model approach. *Clim. Past.* **2007**, *3*, 355–366. [CrossRef]
85. Brewer, S.; Guiot, J.; Torre, F. Mid-Holocene climate change in Europe: A data-model comparison. *Clim. Past.* **2007**, *3*, 499–512. [CrossRef]
86. Mahlstein, I.; Knutt, R. Regional climate change patterns identified by cluster analysis. *Clim. Dyn.* **2010**, *35*, 587–600. [CrossRef]
87. Henríquez, G. *Caracterización de Humedales Altoandinos Para una Gestión Sustentable de las Actividades Productivas del Sector Norte del País: Antecedentes Climáticos III Región de Atacama*; Centro de Información de Recursos Naturales (CIREN): Santiago, Chile, 2013.
88. Janis, M.; Robeson, S. Determining the spatial representativeness of air-temperature records using variogram-nugget time series. *Phys. Geogr.* **2004**, *25*, 513–530. [CrossRef]
89. Ciulache, S.; Ionac, N. Topoclimatic and microclimatic diferences in the Piteşti Town-Area. *Present Environ. Sustain. Environ.* **2008**, *2*, 117–124.

90. Martin, F.; Fileni, L.; Palomino, M.G.; Vivanco, M.G.; Garrido, J.L. Analysis of the spatial representativeness of rural background monitoring stations in Spain. *Atmos. Pollut. Res.* **2014**, *5*, 779–788. [CrossRef]
91. Araya-Osses, D.; Casanueva, A.; Román-Figueroa, C.; Uribe, J.M.; Paneque, M. Climate change projections of temperatura and precipitation in Chile based on statistical downscaling. *Clim. Dyn.* **2020**, *54*, 4309–4330. [CrossRef]